한국공작기계학회논문집 Vol.14 No.3 2005. 6.
Transactions of the Korean Society of Machine Tool Engineers

A Study on CNC Performance Test System using the Dynamometer

Chung Sung Kim*, Chan Ho Lee*, Byung Gyu Park+, Eul Seob Jeong++

(논문접수일 2005. 4. 20, 심사완료일 2005. 5. 10)

Dynamometer를 이용한 CNC제어기 성능평가 시스템 개발

김성청*, 이찬호*, 박병규+, 정을섭++

Abstract

It is difficult to separate those of NC controller from the error of machine tools because the conventional testing methods to inspect the performance are including the errors of moving system, therefore it has been used as the methods that compare the other controllers. Also, it is hard to predict the machine itself errors with the methods assembling the NC controller and moving system on machine because of the variable load conditions. In this study, the performance inspecting system was developed by analyse the axis_rotating properties of servo system finally outputting from NC controller. The axis torque was controlled by motor dynamometer and the rotating position accuracy was measured by this developed system.

Key Words : Performance evaluation, Motor dynamometer, Interpolation accuracy, Grid encoder

1. Introduction

Generally, errors of machine tools are classified by static and dynamic error. The static errors are divided into three types: geometric error, thermal deformation error and other errors resulting from NC and moving system responsible for position control of cutter. The dynamic errors result from the oscillation of machine, chatter and vibration of spindle units. The position of cutter is determined by three(X, Y, Z) axis and the position and velocity of each axis is controlled by the NC.

However, path error between actual data(design) and trajectory by NC-controller is unavoidable and this error is largely influenced by the type of ac and deceleration

---

* Sung-Chung Kim, School of Mechnical Eng., Chungbuk National University (sckim@chungbuk.ac.kr)
Address: #12 Gaesin-dong, Cheongju, Chungbuk,361-763, Korea
+ Computer-aided Mechanical Dept., Juseong Technical College
++ Automobil & Shipbuilding Industry Division, Ministry of Commerce, Industry and Energy

and control method of servo-control system. The existing evaluation system, in which the performance of machine is evaluated by installing NC-controller and servo system on the reference transportation system such as machine tool or X-Y table, should include the error of machine tool or reference transportation system, and makes it difficult to predict the error of machine itself due to the load since defining quantitative measures of load is difficult.

This study tried to examine the whole performance of NC-controller including S/W(G-code) of CNC by moving the NC-controller with various operation orders and measuring encoder signals in real time in order to examine and evaluate the error of NC-controller per second and to contribute for the improvement of performance of the NC machine.

2. Method of Performance Evaluation using Motor Encoder

2.1 Structure of Rotary Encoder

Generally, an optical encoder installed at servo motor of the NC controller detects the quantity of positional transportation, and rotary encoders are divided into incremental and absolute one by its function. Optical encoder is composed of the luminous source, induction element, and rotary disk with slit. The rotary disk between the luminous source and the induction element gives out pulse generating power proportional to rotary angle.

Figure 1 and 2 shows an optical encoder with a fixed slit, in which an LED is used as the luminous source in order to project the light through rotary disk perpendicularly to the induction element. Light(infrared) beamed from LED is detected by the induction element, after passing the slit of rotary disk and the slit of fixed slit plate.

Figure 3 shows the structure of an A, B generating power type incremental encoder with Z-phase signal. Light beamed from LED is detected by the induction element A, B, Z, after passing the slit of rotary disk and each slit corresponding to A, B and Z on the fixed slit plate. The slits A and B on the fixed slit plate are positioned to have an phase difference of 90 degree, and the electrical signal output that is fitted in terms of wave form becomes a rectangular.

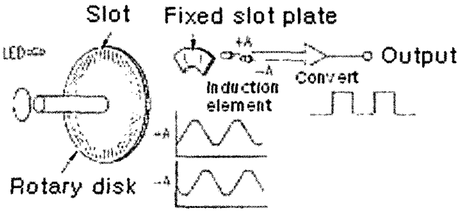

Fig. 1 Optical Encoder

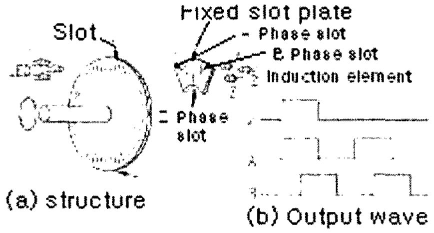

(a) structure (b) Output wave

Fig. 2 Incremental Encoder

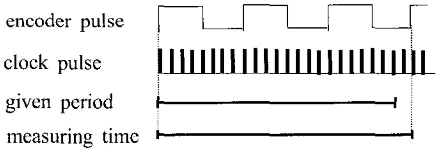

Fig. 3 Principle of speed detection

The incremental encoder has a simple structure, it is cheap, and the signal transmission is simple because of the small number of output lines. The output pulse of encoder does not correspond to the absolute value of the rotating position of axis but the rotation angle of axis. In the case of performance with absolute measures, the output pulse is represented as accumulated counter.

Sufficient measures to prevent noise should be done, since noise is accumulated at the counter in the process of signal transmission. Moreover, special attention to the power supply should be paid, as it is impossible to mark the original position after power shut-down.

Since the incremental encoder generates pulse temperature from itself, the number of output pulse of encoder should be transformed from F/V converter into analog signal that is proportional to the pulse frequency in order to attain the analog signal for detection of the rotational velocity.

In order to measure velocity using rotary encoder, this study measured the pulse frequency of encoder signal instead of F/V converter.

2.2 Measurement of Position and Velocity using Motor Encoder

In this study, the encoder signal of motor was read and processed in order to evaluate the performance of NC transformation control equipment. In order to analyze the performance according to various criteria, CNC gives performance order with the shaft of motor attached at dynamometer. The transportation displacement and velocity were calculated by measuring and conversing the volume of motor rotation transportation as for X, Y, and Z axis.

Measurement of displacement by encoder

We calculated the transportation displacement by reading pulse increment of rectangular wave emitted from encoder through the encoder board with four-time multiplication. The transportation displacement is determined by the number of motor encoder pulse per rotation and the pitch value of ball screw of the transportation axis. In this study, this value was pre-set on the encoder board setting window before the beginning of experiment. An example of setting is as follows:

- number of motor encoder pulse per rotation : 5,000pulse/rev.
- after four-time multiplication 20,000pulse/rev.
- screw pitch : 2 mm
  - ⇒ transportation displacement per one encoder pulse : 0.1 μm

Measurement of transportation velocity by encoder

The transportation velocity of each servo axis may be predicted by observing the number of pulse emitted from encoder for every pre-set sampling time. However, this method cannot be used because of the problem of velocity resolution, as the number of encoder pulse per one rotation is restricted.

For example, at least 10 pulse should appear for the measurement of servo axis with 5,000pulse/rev. by the sampling frequency of 2ms, so the measurable number of encoder pulse is 20,000 pulse after four-time multiplication. In this case, the minimum measurable rotation frequency is calculated with equation (1):

In this case, the minimum measurable transportation velocity becomes 15rpm, and more resolution power is needed for the measurement of velocity control precision of transportation axis.

$$\frac{\dfrac{content\ of\ count}{sampling\ period}\times 60}{no\ of\ encoder} = 15\text{rpm} \qquad (1)$$

Against this background, this study obtained the transportation velocity by measuring the frequency of observed motor encoder. After the number of encoder pulse during the measuring sampling frequency was read, the transportation velocity was calculated by reading the number of clock pulse with the help of an external counter installed at encoder board. Encoder and clock pulse is counted by the counter with leading edge of encoder pulse at respective starting point. The counting is stopped at the first leading edge after the measurement frequency T. In this case, the transportation velocity N is obtained in the following way:

$$N = K \cdot \frac{P_e}{P_c} \qquad (2)$$

Where, Pe is the number of encoder pulse counted during the sampling frequency, Pc is the number of clock pulse, and K is transformation constant. In order words, the transportation velocity of each axis was calculated by using the frequency of encoder pulse during one measurement frequency, which was obtained by reading both encoder and clock pulse simultaneously.

2.3 The Construction of Performance Evaluation System

The measuring and analyzing system used in this study was an PC-based overall performance evaluation system for the performance measurement of NC-controller before the installation of machine, which consists of hardware (CNC, PC, servo motor, dynamometer, interface board etc.) and windows-based user software installed at PC.

The NC-controller was moved with motor and driver, and each servo motor was installed at dynamometer to make the axis torque control possible.

3. Measurement of Precision according to Load

3.1 Position Control Precision

The experiment of position control precision evaluated the performance of position control by comparing the position order by NC-controller with the actual transportation position of servo axis.

Figure 5 shows the result of five-time iterative experiments in the case of an independently moving servo transportation axis. The position control in the both positive and negative direction was performed at the same time, and the results of position control were measured and simultaneously analyzed.

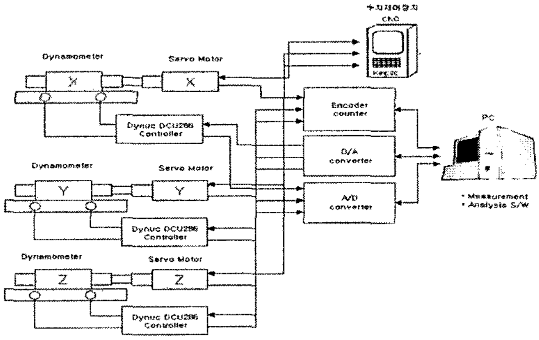

Fig. 4 The equipment for experimenting and analyzing the control precision with motor encoder

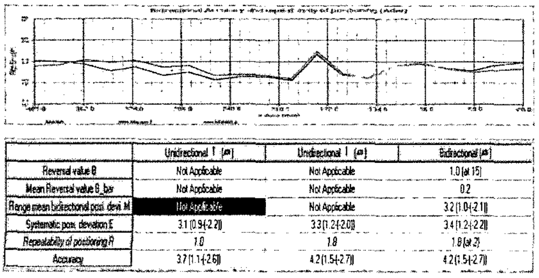

	Unidirectional ↑ (㎛)	Unidirectional ↓ (㎛)	Bidirectional (㎛)
Reversal value B	Not Applicable	Not Applicable	1.0 (at 15)
Mean Reversal value B_bar	Not Applicable	Not Applicable	0.2
Range mean bidirectional posi. devi. M	Not Applicable	Not Applicable	3.2 (1.0(-2.1))
Systematic posi. deviation E	3.1 (0.9(-2.2))	3.3 (1.2(-2.0))	3.4 (1.2(-2.2))
Repeatability of positioning R	1.0	1.8	1.8 (at 2)
Accuracy	3.7 (1.1(-2.6))	4.2 (1.5(-2.7))	4.2 (1.5(-2.7))

Fig. 5 Results of both-direction experiments & analyses

3.2 Contouring Control Precision

Linear Interpolation Transportation Precision

The examination of linear interpolation precision tested the degree with which the actual path of tool movement coincides with the standard linear path, if two or more axis of the NC-controller are moving in the same direction at the same time.

We conducted experiments on two servo axis with varying control parameters of NC-controller and experiment conditions. We performed linear interpolation control with varying test conditions, analyzed the data from motor encoder, and summarized the contouring and maximum error in the normal state.

Circular interpolation transportation precision

At the experiment on the circular interpolation precision, mutual movement of two axes was measured, which includes the case in which the velocity of one of the two linear axes decreases to 0 and the moving direction is changed. We conducted experiments with varying control parameters of NC-controller and experimental conditions. Table 1 summarizes the final experimental results with various conditions. The considered conditions were the radius of circular interpolation, the gain of position controller, time-constant of ac- and deceleration, feed rate, etc.

Free-curved surface precision

The examination of free-curved surface precision was destined to evaluate the characteristics of dynamic movement of NC-machine by measuring two-dimensional random contour. For this purpose, the experiment path and tran-

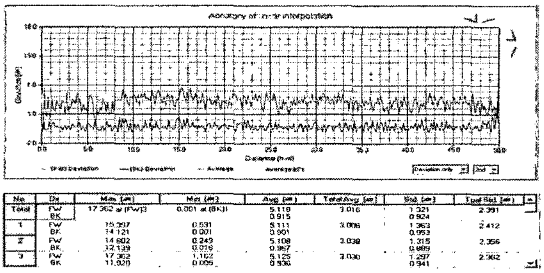

No	Dir	Max (㎛)	Min (㎛)	Avg (㎛)	Total Avg (㎛)	Std (㎛)	Total Std (㎛)
Total	FW BK	17.362 at (FW)3	0.001 at (BK)1	5.118 0.915	3.016	1.321 0.924	2.391
1	FW BK	15.397 14.121	0.531 0.001	5.111 0.901	3.006	1.363 0.953	2.412
2	FW BK	14.602 12.139	0.249 0.016	5.108 0.967	3.038	1.315 0.889	2.356
3	FW BK	17.362 11.920	1.162 0.005	5.125 0.936	3.030	1.297 0.941	2.362

Fig. 6 Results of the experiments on linear interpolation control precision

sportation velocity were defined as a combination of linear and circular interpolation on a two-dimensional plane, and maximum and average contour error were evaluated.

Figure 9 shows the results of contour control experiments for two types of free-curved paths. First of all, contour control error for a path with the combination of circular and linear interpolation. At first, contour control error on the path with combination of circular and linear interpolation is shown. The measured coordination value of transportation and the calculated contour error at this point are listed in table. Moreover, Figure 9 describes the maximum and average error and standard deviation at the all points on the path.

Table 1 Change of radius by experimental conditions

Exp. Type	Radius	Feedrate (mm/min)	Position Gain	Time-constant at ac- and deceleration	Least Square R(mm)	Radial Dev. (μm)	Circular Dev. (μm)	Change of Radius (μm)
Change of feed rate	25mm	250	X,Y= 2500	50	25.0000	6.9, -11.4	18.3	0.0
		500			24.9965	1.1, -10.3	11.4	-3.5
		750			24.9904	-4.4, -21.8	17.4	-9.6
		1000			24.9817	-12.2, -34.2	22.1	-18.3
		1250			24.9707	-21.2, -46.9	25.7	-29.3
		1500			24.9570	-31.6, -63.2	31.6	-43.0
		1750			24.9409	-46.1, -78.9	32.9	-59.1
Change of P gain	25mm	500	1000	〃	24.9856	-6.7, -26.4	19.8	-14.4
			1500		24.9930	-0.9, -17.7	16.7	-7.0
			2000		24.9955	0.8, -12.6	13.4	-4.5
			2500		24.9965	1.3, -13.3	14.6	-3.5
			3000		24.9970	1.9, -13.3	15.2	-3.0
			3500		24.9974	6.2, -13.9	20.2	-2.6
			4000		24.9975	2.7, -12.5	15.2	-2.5
Change of time-constant at ac- and deceleration	25mm	500	X,Y= 2500	25	24.9990	4.5, -12.3	16.8	-1.0
				50	24.9965	1.1, -10.3	11.4	-3.5
				75	24.9923	-2.8, -17.2	14.4	-7.7
				100	24.9861	-6.5, -26.0	19.5	-13.9
				125	24.9783	-15.6, -33.6	18.0	-21.7
				150	24.9687	-24.0, -41.0	17.0	-31.3
				175	24.9575	-37.3, -52.7	15.5	-42.5
				200	24.9446	-48.5, -66.6	18.1	-55.4
Change of radius	10	500	X,Y= 2500	50	9.9888	-5.6, -19.8	14.1	-11.2
	25				24.9965	1.1, -10.3	11.4	-3.5
	35				34.9981	4.1, -10.8	14.9	-1.9
	50				49.9999	7.7, -7.2	14.9	-0.1
	60				60.0006	5.7, -8.9	14.6	0.6
	75				75.0017	8.4, -8.0	16.4	1.7
	100				100.0032	10.5, -6.8	17.2	3.2

4. Comparing Measurement with Grid Encoder

4.1 Structure of Grid Encoder

Grid encoder is an non-contact type measuring equipment, which is appropriate for measuring dynamic precision of very small circles with high axis acceleration.

In this study, the actual performance of a system with NC-controller and transportation system was evaluated by using grid encoder, and the results were compared with the results obtained by using motor encoder, with the aim of improving system performance by isolating the error of controller per se from the error of transportation system. KGM182 grid encoder by Heidenhain Co., which was used in this study, consists of a lattice circular plate with waffle-form scales(diameter 230mm) fixed at mounting base and a non-contact scanning head, whose structure is shown in Figure 10. This equipment

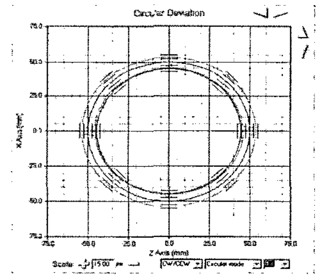

Fig. 7 Experimental Results of Circular deviation (circular mode)

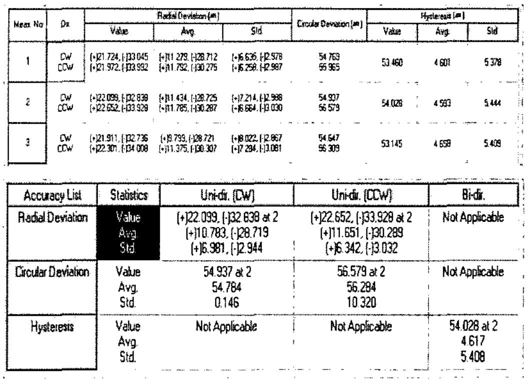

Meas. No	Dir.	Radial Deviation (μm) Value	Radial Deviation (μm) Avg.	Radial Deviation (μm) Std.	Circular Deviation (μm)	Hysteresis (μm) Value	Hysteresis (μm) Avg.	Hysteresis (μm) Std.
1	CW CCW	(+)21.724, (-)33.045 (+)21.972, (-)33.992	(+)11.279, (-)28.712 (+)11.792, (-)30.275	(+)6.636, (-)2.976 (+)6.258, (-)2.987	54.763 55.965	53.460	4.601	5.378
2	CW CCW	(+)22.099, (-)32.838 (+)22.652, (-)33.928	(+)11.434, (-)28.725 (+)11.785, (-)30.287	(+)7.214, (-)2.986 (+)6.664, (-)3.030	54.937 56.579	54.028	4.583	5.444
3	CW CCW	(+)21.911, (-)32.736 (+)22.301, (-)34.008	(+)9.799, (-)28.721 (+)11.375, (-)30.307	(+)8.022, (-)2.867 (+)7.284, (-)3.081	54.647 56.309	53.145	4.658	5.408

Accuracy List	Statistics	Uni-dir. (CW)	Uni-dir. (CCW)	Bi-dir.
Radial Deviation	Value Avg. Std.	(+)22.099, (-)32.838 at 2 (+)10.783, (-)28.719 (+)6.981, (-)2.944	(+)22.652, (-)33.928 at 2 (+)11.651, (-)30.289 (+)6.342, (-)3.032	Not Applicable
Circular Deviation	Value Avg. Std.	54.937 at 2 54.784 0.146	56.579 at 2 56.284 10.320	Not Applicable
Hysteresis	Value Avg. Std.	Not Applicable	Not Applicable	54.028 at 2 4.617 5.408

Fig. 8 Final Results of Circular Interpolation Experiment

can measure the radius from minimum 1㎛ to maximum 115mm at the maximum velocity of 80,000mm/min.

This grid encoder is a kind of ultra-precision lattice interferometers using single LED, which are known to enable more precise measurement because they are less sensitive to the changes of temperature or humidity compared to laser interferometer and more resistant to noise compared to electro-magnetic scale.

When the grid encoder is installed at the machine tool, an installation error is unavoidable, which means that two axes of encoder do not coincide with two axes of measured machine. In this case, the installation error can be compensated by transforming the coordinate of present position P(x_0, y_0) read from the sensor into(x_0', y_0') for machine coordinate by rotation.

$$\begin{bmatrix} x_0' \\ y_0' \end{bmatrix} = \begin{bmatrix} \cos\theta & \sin\theta \\ -\sin\theta & \cos\theta \end{bmatrix} \begin{bmatrix} x_0 \\ y_0 \end{bmatrix} \tag{3}$$

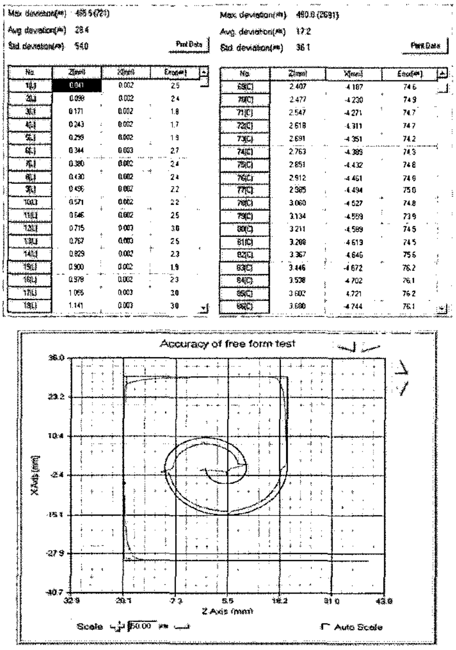

Max deviation(㎛) 465.5(721)
Avg deviation(㎛) 28.4
Std. deviation(㎛) 54.0

No.	Z(mm)	X(mm)	Error(㎛)
1(L)	0.041	0.002	2.5
2(L)	0.098	0.002	2.4
3(L)	0.171	0.002	1.8
4(L)	0.243	0.002	1.7
5(L)	0.299	0.002	1.9
6(L)	0.344	0.003	2.7
7(L)	0.380	0.002	2.4
8(L)	0.430	0.002	2.4
9(L)	0.496	0.002	2.2
10(L)	0.571	0.002	2.2
11(L)	0.646	0.002	2.5
12(L)	0.715	0.003	3.0
13(L)	0.767	0.003	2.5
14(L)	0.829	0.002	2.3
15(L)	0.900	0.002	1.9
16(L)	0.978	0.002	2.3
17(L)	1.065	0.003	3.0
18(L)	1.141	0.003	3.0

Max. deviation(㎛) 490.8(2691)
Avg. deviation(㎛) 17.2
Std. deviation(㎛) 36.1

No.	Z(mm)	X(mm)	Error(㎛)
69(C)	2.407	-4.187	74.6
70(C)	2.477	-4.230	74.9
71(C)	2.547	-4.271	74.7
72(C)	2.618	-4.311	74.7
73(C)	2.691	-4.351	74.2
74(C)	2.763	-4.389	74.3
75(C)	2.851	-4.432	74.8
76(C)	2.912	-4.461	74.9
77(C)	2.985	-4.494	75.0
78(C)	3.060	-4.527	74.8
79(C)	3.134	-4.559	73.9
80(C)	3.211	-4.589	74.5
81(C)	3.288	-4.619	74.5
82(C)	3.367	-4.646	75.6
83(C)	3.446	-4.672	76.2
84(C)	3.538	-4.702	76.1
85(C)	3.607	4.721	76.2
86(C)	3.680	-4.744	76.1

Fig. 9 Examination and Analysis of Free-Curved Surface Transportation Precision

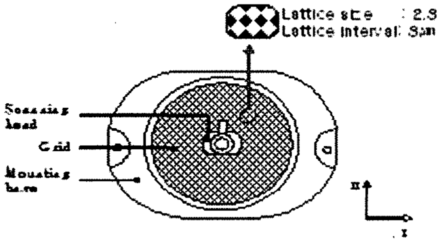

Fig. 10 Structure of Grid Encoder

4.2 Construction of Comparing System

Figure 11 shows the construction of control precision test equipment using motor and grid encoder, and Figure 12 shows the grid encoder and experiment equipment installed on the X-Y table with NC-controller and transportation system.

4.3 Measuring Experiment and Results

Figure 13 and 14 show the results of circular interpolation transportation precision test with a radius of 50mm and velocity of 1000mm/min and the error data and the results of error diagnostics in the developed system.

Figure 15 is an on-line measurement screen by the developed system for the measurement of corner-cutting precision. display screen and shows the results of analyses of the contour error at corner transportation.

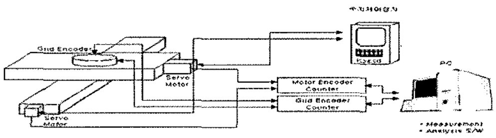

Fig. 11 Construction of control precision test equipment using motor and grid encoder

Fig. 12 Schematic diagram of Grid Encoder System

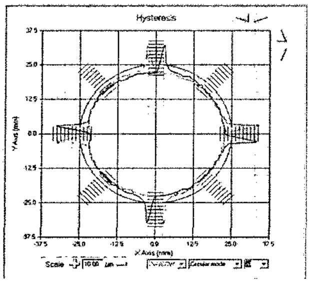

Fig. 13 Test result of circular interpolation

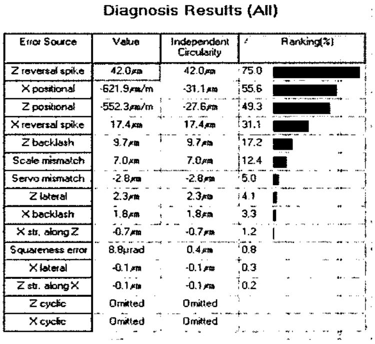

Diagnosis Results (All)

Error Source	Value	Independent Circularity	Ranking(%)
Z reversal spike	42.0μm	42.0μm	75.0
X positional	-621.9μm/m	-31.1μm	55.6
Z positional	-552.3μm/m	-27.6μm	49.3
X reversal spike	17.4μm	17.4μm	31.1
Z backlash	9.7μm	9.7μm	17.2
Scale mismatch	7.0μm	7.0μm	12.4
Servo mismatch	-2.8μm	-2.8μm	5.0
Z lateral	2.3μm	2.3μm	4.1
X backlash	1.8μm	1.8μm	3.3
X str. along Z	-0.7μm	-0.7μm	1.2
Squareness error	8.8μrad	0.4μm	0.8
X lateral	-0.1μm	-0.1μm	0.3
Z str. along X	-0.1μm	-0.1μm	0.2
Z cyclic	Omitted	Omitted	
X cyclic	Omitted	Omitted	

Fig. 14 Error analysis of circular interpolation

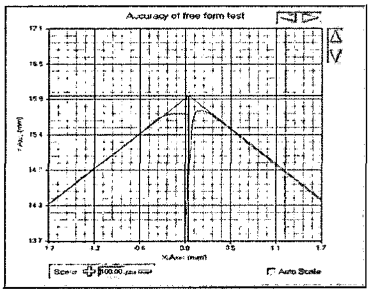

Fig. 15 Corner moving accuracy

4. Conclusion

In this study, we controled the axis torque precisely by using motor dynamometer in order to analyze the characteristics of shaft rotation of servo system finally produced from the servo system of NC-controller, and we developed an performance test equipment that covers the overall performance of NC-controller including moving S/W(G-code) by measuring the degree of precision of rotation position.

Using the developed system, the pure error of NC-controller was evaluated by measuring motor encoder signals according to load conditions before the installation of servo system. Moreover, we tried to contribute to improving the performance of controller as well as transportation system by comparing the results of grid encoder measurement, in which the final precision is measured by attaching NC-controller and servo system at machine tool or standard transportation system, as currently used. with the aim of distinguishing the error of NC-controller per se from the error of transportation system.

Finally, this study aims to increase reliability of NC-controller, which still makes out a weak point in domestic machine tool industry, and to enhance technological competitiveness.

Acknowledgement

This work was supported by the research grant of the Chungbuk National University in 2004. Thanks to all person concerned with this project.

Reference

(1) Poo, A., and Bollinger, J., 1972, "Dynamic Errors in Typical Contouring System," *IEEE Trans. of Industry Application*, Vol. 1A-8, No. 4.

(2) ISO, 1996, *ISO 230-4 Test code for machine tools - part 4: Circular tests for numerically controlled machine tools*, First edition.

(3) Knapp, W., 1983, "Test of the Three-dimensional Uncertainty of Machine Tools and Measuring Machines and its Relation to the Machine Errors," *Annals of the CIRP*, Vol. 32, No. 2, pp. 459~464.

(4) Bryan, J. B., 1982, "A Simple Method for Testing Measuring Machines and Machine Tools, Part 1: Principle & applications," *Precision Engineering*, Vol. 4, No. 2, pp. 61~69.

(5) Kakino, Y., Ihara, Y., Nakatsu, Y. and Okamura K., 1987, "The Measurement of Motion errors of NC Machine Tools and Diagnosis of their Origins by using Telescoping Magnetic Ball Bar Method," *Annals of CIRP*, Vol. 36, pp. 377~380.